

## DISCUSSION

**Cahn, R. W.:** Your postulate that the observed increase of resistivity at quite low temperatures is due to dissociation of solute-vacancy pairs is, on the face of it, reasonable. Since, however, the pairs formed during a quench (*i.e.* at quite high temperatures presumably), I can not understand why the pairs should "want" to dissociate at low temperatures. Could Dr. Quéré elucidate?

**Quéré, Y.:** The peculiar point, indeed, shown by the trapping calculation is rather that, after a slow quench, one can reach the equilibrium value of complexes at room temperature. If this is true, it is then normal that the complexes should dissociate as soon as heated though the binding energy here proposed is perhaps surprisingly high.

**Tomizuka, C. T.:** In view of difficulty Drs. Doyama and Koehler had with quenching-in vacancies in silver, I would like to hear the views of Prof. Koehler.

**Koehler, J. S.:** We attempted to be very careful to be certain that no oxygen was present in our silver. We believe that the oxygen concentration in our specimens was less than one part in  $10^7$ . The experiments of Quéré show the behavior of silver containing oxygen.

PROCEEDINGS OF THE INTERNATIONAL CONFERENCE ON CRYSTAL LATTICE DEFECTS, 1962, CONFERENCE JOURNAL OF THE PHYSICAL SOCIETY OF JAPAN VOL. 18, SUPPLEMENT III, 1963

## Effect of Solute Atoms upon Vacancy Climb of Prismatic Dislocations in Al-5% Mg Alloy

A. EIKUM AND G. THOMAS

*Department of Mineral Technology and Inorganic Materials Research Division  
Lawrence Radiation Laboratory, University of California, Berkeley, U.S.A.*

The climb rate of prismatic dislocations in quenched Al-5% Mg alloy has been studied by bulk annealing and also by high temperature electron microscopy of thin foils. In bulk and thin foil specimens loops and helices are always observed to grow. The activation energy is determined to be  $0.95 \pm 0.05$  eV. The results can be understood on the basis of a binding energy between vacancies and magnesium atoms which can be  $\sim 0.1$ – $0.4$  eV, depending upon their geometrical configuration.

### Introduction

Since the fraction of vacant atom sites in metals increases with temperature by the relationship  $A \exp(-E_f/kT)$  where  $A$  is an entropy factor ( $\sim 1$ ),  $E_f$  the energy of formation ( $\sim 1$  eV) of a vacancy and  $k$  is Boltzmann's constant, very large vacancy supersaturations are possible by quenching rapidly from near the melting point (*e.g.*,  $\sim 10^9$  for pure Al<sup>1)</sup>). Upon aging after quenching, supersaturation can be eliminated by migration of vacancies to sinks (surfaces, grain boundaries, etc.) or

by vacancy clustering to form dislocation loops or other defects. The vacancy migration energy,  $E_m$ , is the energy barrier for an atom to jump into an adjacent vacant site. The sum of  $E_m$  and  $E_f$  is the self diffusion energy  $E_D$ .

Values of  $E_D$  are usually obtained from isothermal resistivity measurements but can also be obtained from direct measurements of the isothermal change in size of dislocation loops using electron microscopy techniques. (For review see Whelan.<sup>2)</sup>) In two

component systems if solute atoms and vacancies are bound with an energy  $E_B$  the value of  $E_D$  may be altered because the migration energy in the alloy is then  $E_m + E_B$ .  $E_B$  may also change  $E_f$ , as suggested *e.g.* by the differences in dislocation loop densities observed in pure metals and their alloys.<sup>31</sup> It is found that in quenched Al alloys loop formation is usually inhibited and helical dislocations, resulting from the vacancy climb of screw dislocations, are the predominant defects.<sup>31,41</sup> It has been concluded that solute atoms are associated with vacancies, thereby hindering the elimination of vacancy supersaturation. Estimates of  $E_B$  for the systems Al-Zn<sup>51</sup>, Al-Cu<sup>61</sup> and Al-Ag<sup>71</sup> have already been made, and in this paper we have estimated  $E_B$  in Al-5% Mg from direct measurements of the change in size of loops using high temperature transmission electron microscopy.

### Experimental

Annealed Al-5% Mg alloys (total impurity (Mg+Cu+Si+Fe+Mn)=0.02%) in the form of 4 ins.  $\times$  1 in.  $\times$  0.005 ins. thick strip were quenched into iced brine ( $-15^\circ\text{C}$ ) or water at  $80^\circ\text{C}$  after  $\frac{1}{2}$  hour solution heat treatment at  $550^\circ\text{C}$ . Thin foil specimens prepared after quenching showed no noticeable differences in structure when examined in a Siemens Elmiskop lb microscope (foils were prepared by electropolishing in the usual way). After quenching, specimens were kept at room temperature for 24 hours before being examined in the microscope. Bulk annealing was done at  $100^\circ$ ,  $183^\circ$  and  $300^\circ\text{C}$  for various times. Annealing of thin foils was done in the electron microscope using a Siemens hot-stage with which the temperature can be estimated to within  $\pm 10^\circ\text{C}$ . Dynamic changes

in the foils were recorded on 16 mm Tri-X film using a Bolex Cine camera fitted with a Bell and Howell f 0.95 lens (used wide open). The film speed employed was 10 frames/sec.

### Results

#### (1) As-Quenched Structure

In a given specimen prepared after quenching and aging at  $20^\circ\text{C}$  adjacent regions contain poorly developed helices, uniform helices, random loops and columns of prismatic loops (Fig. 1). This structure is typical of quenched Al-alloys.<sup>31</sup> Contrast experiments show that the loops are prismatic  $a/2\langle 110 \rangle$  dislocations and the axes of the helices are parallel to  $\langle 110 \rangle$ . The average diameter of helices was  $483\text{\AA}$  with  $7 \times 10^{13}$  turns/cm<sup>3</sup>. Thus, for a foil  $5000\text{\AA}$  thick the vacancy concentration  $x'$  is  $3.7 \times 10^{-5}$  ( $x' = \pi R^2 b N$  where  $R$  is loop radius,  $b$  its Burgers vector,  $N$  density of loops). The vacancy concentration  $x'$  calculated for loops was  $3.6 \times 10^{-5}$  (see Table I). These values are somewhat smaller than those previously determined for Al-Mg alloys<sup>31</sup> and are an order of magnitude lower than  $x$  for pure aluminum.<sup>81</sup> A specimen of Al-5% Mg alloy was deformed immediately after quenching to 3% strain and aged 11 minutes

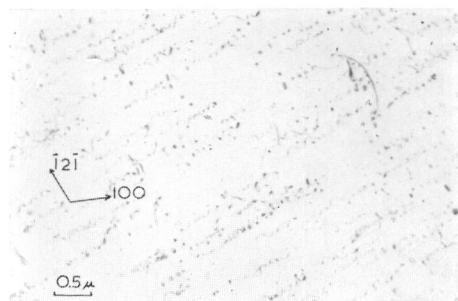


Fig. 1. Al-5% Mg quenched from  $550^\circ\text{C}$  into ice-brine and aged at  $20^\circ\text{C}$ .

Table I. Vacancy concentrations in Al-5% Mg after quenching and aging; all specimens initially quenched into iced brine.

Treatment	Helices			Loops		
	$\frac{\text{Turns}}{\text{cm}^3}$	Dia., $\text{\AA}$	Vac. Conc.	$\frac{\text{Loops}}{\text{cm}^3}$	Dia., $\text{\AA}$	Vac. Conc.
550°C Q. + 24 hr. 20°C Average	$7.1 \times 10^{13}$	483	$3.7 \times 10^{-5}$	$1.2 \times 10^{14}$	360	$3.6 \times 10^{-5}$
550°C Q. + 60' 183°C Average	$1.1 \times 10^{13}$	2740	$1.9 \times 10^{-4}$	$1.4 \times 10^{13}$	2890	$2.6 \times 10^{-4}$
Single large defect	$7.1 \times 10^{12}$	6250	$6.3 \times 10^{-4}$	$3.6 \times 10^{12}$	6250	$3.1 \times 10^{-4}$
550°C Q. 3% el. aged 11' 20°C + 8% el.	—	—	—	$6.9 \times 10^{12}$	4400	$3.0 \times 10^{-4}$

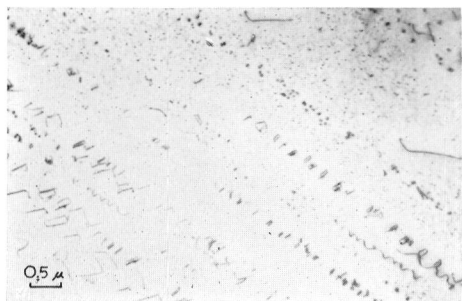


Fig. 2. Al-5% Mg quenched from 550°C into ice-brine. Deformed immediately 3% and aged 11 min. at 20°C followed by extension to 11% total elongation.

at 20°C. The strain was then increased to 11% total. As shown in Fig. 2, the loop density has increased and the vacancy concentration is now determined to be  $3 \times 10^{-4}$ . This experiment shows that although many vacancies have annealed out during quenching or room temperature aging, a relatively high concentration is still retained in "solid solution" and some fraction of these seem to be released by cold work.

### (2) Aged Bulk Specimens

The density of loops was observed to decrease upon aging but their diameter increased, *e.g.*, to  $\sim 3000 \text{ \AA}$  after 60 min. at 183°C. In many cases coalescence of loops occurred. The concentration of vacancies calculated from the size and density of loops and helices is shown in Table I. The values of  $x'$  are again 10 times that for the as-quenched specimen. Helical dislocations also grew and became aligned in  $\langle 110 \rangle$ . Eventually they often degenerated into large loops. The only indication of precipitation was obtained after annealing for 50 hours above 150°C and furnace cooling, after which treatment, small precipitates could be observed only in grain boundaries. At no time was precipitation observed in the matrix.

### (3) Annealing of Foils

The annealing of bulk specimens showed that loops are much more stable than those in pure aluminum and that helices are preserved to relatively high temperatures. Under the aging treatments used here, helices do not appear to be preferential sites for precipitation as they are in Al-4% Cu.<sup>9)</sup> Aging thin foils in the high temperature stage always resulted in loop and helical

dislocation growth at all temperatures (100–400°C), as shown in Fig. 3; whereas in thin foils of pure Al, loops are always observed to shrink and eventually disappear at  $\sim 200^\circ\text{C}$  as vacancies are lost to the surfaces.<sup>10)</sup> The kinetic data show that the rate of growth  $dr/dt$  was a constant even when a loop intersected the foil surface, *e.g.*, at A, Fig. 3(a). This rate is shown in Fig. 4 as a function of temperature (for  $T > 250^\circ\text{C}$ ) and represents

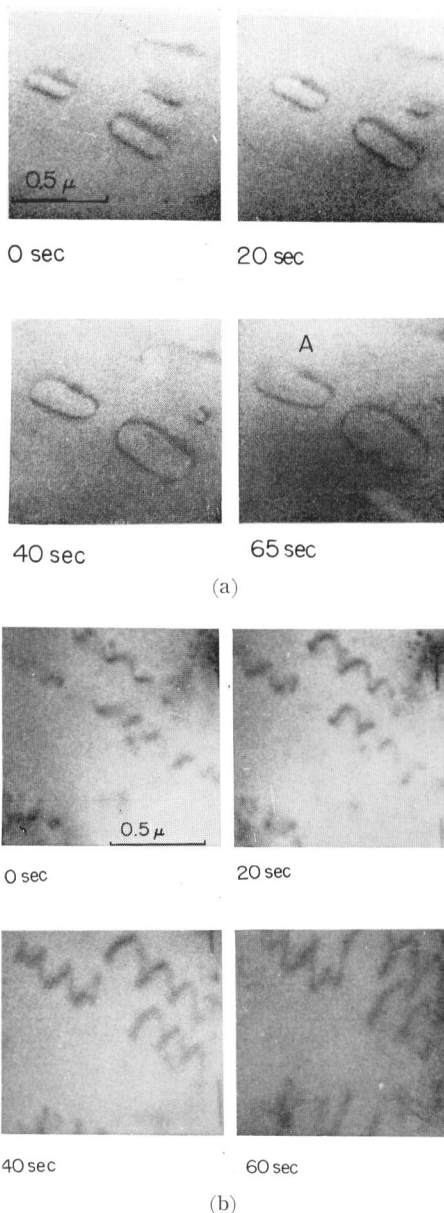


Fig. 3. Heating stage time sequence showing, (a) Loops growing at 365°C and (b) Helices growing at 280°C.

measurements of loop growth with initial radii varying from 200 to 1500 Å. The activation energy  $E'_G$  of the process is  $0.95 \pm 0.05$  eV as compared to the value  $E_{-G} = 1.3$  eV for pure Al.<sup>10)</sup> This result immediately suggests that a strong vacancy-magnesium atom(s) binding energy exists. During loop growth, no loops were observed to shrink except *once* only where the activation energy was found to be 1.3 eV (Fig. 5), *i.e.*, the same value as in pure Al. This loop must therefore be a chance case for an effect near the surface and away from the influence of Mg atoms.

The calculation of  $E'_{-G}$  for the shrinking loop was made using the analysis of Silcox and Whelan.<sup>10)</sup> The time  $t$  for a given loop

to shrink to  $r=0$  is related to  $E'_{-G}$  by:

$$t = t_0 \exp\left(\frac{E'_{-G}}{kT}\right)$$

where

$$t_0 = r_0^2 (z\nu b^2 \alpha)^{-1}$$

$z$  is the coordination number (11),  $\nu$  the atomic frequency factor ( $\sim 10^{13}$ ),  $b = 2.86 \text{ \AA}$  and  $\alpha$  was estimated from the above work<sup>10)</sup> to be  $\sim 50$ .

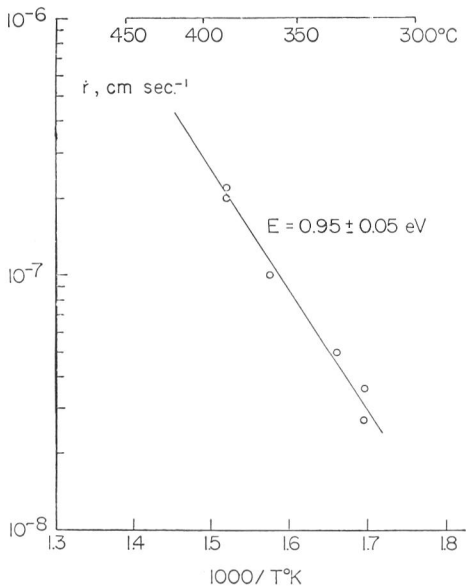


Fig. 4. Rate of increase in loop radius vs reciprocal of the absolute temperature.

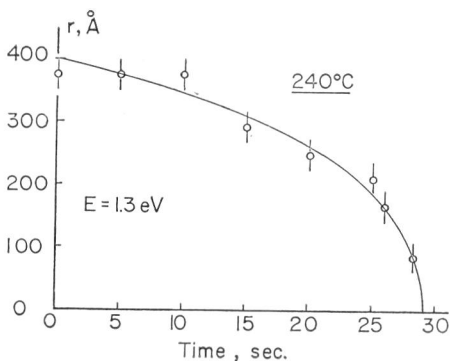


Fig. 5. Decrease in radius with time at 240°C.

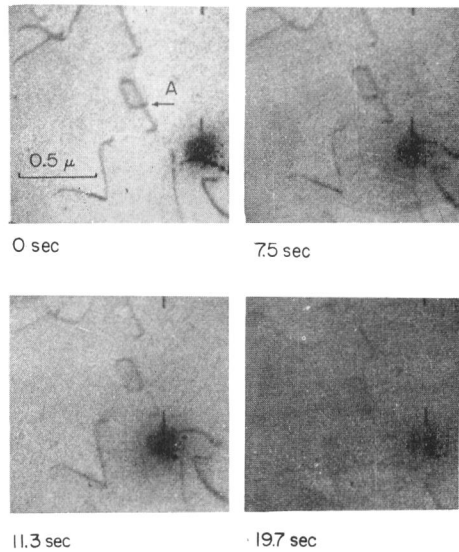


Fig. 6. Possible loop formation from single helical turn in thin foil at 280°C.

Kinetic data for growth of helices is not yet available. However, helices also grew and became more angular following  $\langle 110 \rangle$ . Eventually helices break up into large loops (Fig. 6) which then grow with an activation energy, again  $\sim 0.95$  eV.

### Discussion

#### (1) The Binding Energy

The increase in the vacancy concentration upon aging compared to that for the quenched specimen (Table I) indicates that after quenching, specimens still contain supersaturated vacancies. It is reasonable to suppose that these are bound to magnesium atoms (in some way) as this can account for the low activation energy for climb in the Al-Mg alloy compared to pure Al.

The vacancy concentration  $x'$  in a two component system is given by the following:<sup>11)</sup>

Table II.

Specimen Treatment	$\frac{x'}{x}$	$E_B$
Q 550° and aged 60' at 183°C		
Av. both loops and helices	2.3	0.08 eV
Single large loop	3.1	0.10
Single large helix	6.3	0.16
Q 550°C and strain-aged at 20°C		
Column of large loops	3.0	0.10

$$x' = A \exp\left\{\frac{-E_f}{kT}\right\} \times \left[1 - 12c + 12c \exp\left\{\frac{E_B}{kT}\right\}\right]$$

where  $E_f$  is the vacancy formation energy in the pure metal and  $c$  is the atomic fraction of solute atoms.

Since  $x'$  is measured and  $x$  for the pure metal can be calculated from  $x = A \exp\{-E_f/kT\}$ , the ratio  $x'/x$  can be used to estimate  $E_B$ , since

$$\exp\left(\frac{E_B}{kT}\right) = \left[\left(\frac{x'}{x} - 1\right) + 12c\right] \frac{1}{12c}.$$

Values of  $x'/x$  and  $E_B$  were calculated for the  $x'$  values shown in Table I and the results are shown in Table II.

The binding energies are thus between 0.1 and 0.2 eV. For  $E_B = 0.1$  eV the ratio

$$\frac{\text{Mg atoms—vacancies}}{\text{Al atoms—vacancies}}$$

is  $10^2$  at 20°C, *i.e.*, about  $1 \times 10^{-5}$  unassociated vacancies are present after quenching. This is about the value that is measured (Table I), so presumably these are the vacancies which first condense to loops or onto screw dislocations causing climb into helices.

The remaining vacancies are thus probably bound to magnesium atoms; in the simplest case as a Mg-vacancy pair or as a more complex but stable Mg-vacancy group, *e.g.*, in Mg atom clusters\* which cannot be resolved in the electron microscope. With this in mind one can envisage the aging sequence as follows: free vacancies → loops and helices;

\* Since the precipitates  $\text{Mg}_3\text{Al}_2$  in Al-Mg alloys form under compression, they are expected to be a vacancy sink so that prior to precipitation groups of magnesium atoms are expected to collect vacancies.

vacancies + magnesium atoms → pairs or clusters; vacancies ( $\pm$  Mg atoms) → loop, helix growth. The bound vacancies thus provide the flux necessary for the growth of loops. In pure Al, only free vacancy diffusion occurs and loops can grow only by competition with other loops.<sup>12)</sup> If the vacancy-magnesium pairs provide the vacancy sources for loop growth, the energy  $E'_G$  is  $E_m + E_B$  and does not include  $E_f$ . Thus taking  $E_D = 1.3$  eV for pure Al,  $E_m = 0.54$  eV,<sup>13)</sup> and  $E'_G = 0.95$  eV, the maximum value for  $E_B$  is 0.4 eV. On the other hand, if vacancies are "lost" in some complex configuration with Mg atom clusters,  $E'_G = E_f + E_m - 2E_B$ , assuming that  $E_B$  is equally effective on  $E_f$  and  $E_m$ . Taking the same values for  $E'_G$ ,  $E_D$ ,  $E_f$  and  $E_m$  given above,  $E_B$  is then 0.17 eV, which is in good agreement with the values obtained in Table II. Thus, our results can be best understood on the basis that excess vacancies are bound up in some complex cluster with magnesium atoms. Besides the two extreme cases considered here,  $E_B$  may have any value between 0.1 and 0.4 eV depending upon the geometrical configuration of the Mg-vacancy group.

The Mg-vacancy attraction is explainable in the simplest way in terms of the relief of elastic strains. Since the Mg atom is ~14% larger than an Al atom and a vacancy is thought to be 40% smaller than an atom,<sup>17)</sup> combination of Mg atoms and vacancies might be expected. One can also envisage a similar effect at edge dislocations, *e.g.*, prismatic loops and parts of helices. Here, Mg atoms might sit preferentially on the tension side and vacancies on the compression side of the dislocation. Thus one might expect a local supersaturation of Mg atoms and vacancies around the dislocations, so that they are

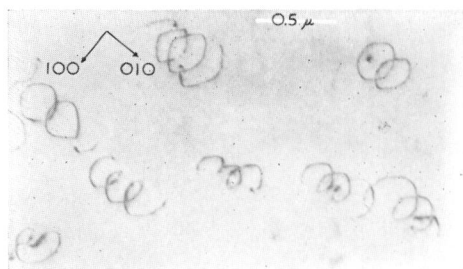


Fig. 7. Al-5% Mg, quenched from 550°C and aged 60 min. at 183°C.

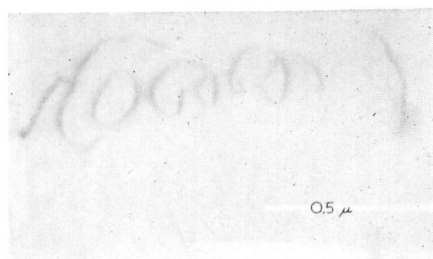


Fig. 9. Al-5% Mg, quenched and aged 60 min. at 183°C.

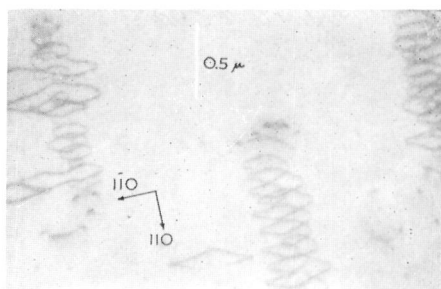


Fig. 8. Al-5% Mg, quenched from 520°C and aged 94 hrs. at 100°C.

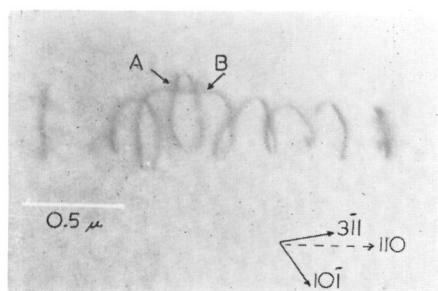


Fig. 10. Al-5% Mg, quenched and aged 60 min. at 200°C.

effectively trapped. This is consistent with the observation that helices become angular, or increase their edge component, during isothermal annealing, *e.g.*, Figs. 7 and 8.

A further check on the value of  $E_B$  is being made by determining the actual value of  $E_f$  for the alloy from electrical resistivity experiments.

## (2) Growth of Helices

Columns of prismatic dislocation loops which are observed in quenched Al-5% Mg (Fig. 1) appear to have formed from helices by some mechanism. The interaction of a gliding dislocation with a helix, and the interaction of adjacent helices of opposite sign have been discussed.<sup>4), 14)~16)</sup> The latter interaction results in prismatic loops having twice the diameter of original helices as is found in electron micrographs. One would also expect to find some trace of moving dislocations after the first type of reaction had occurred. These mechanisms do not appear to account for many of the present observations.

One example of a loop which has formed within helices is shown in Fig. 9. Here one can observe the segment of dislocation which is repelled by the loop after the helix degenerates. Fig. 10 shows a helix along which

adjacent line segments appear ready to combine at A. The straight segment, B, is parallel to the [110] trace and may be pure screw. These results, together with Fig. 6, imply that the degeneration of helicoidal lines into prismatic loops can occur without interaction with a second dislocation.

The three cases illustrated in Figs. 9 and 10 show helices which are not uniformly developed, a feature which may be important in loop formation. Local fluctuations in vacancy or solute atom concentration, or stress fields may allow one segment of helix to climb at a faster rate than neighboring segments. A larger than normal turn, having a larger radius of curvature, should be less stable under existing stress fields.

The effectiveness of stress in the process of forming columns of loops may be more important during quenching. Data in Table I indicate equivalent vacancy concentrations for both helices and columns of loops after the quench and 20°C age. Therefore, if the concentrations are reasonably accurate, one would expect that columns of loops originated from helices by a combined climb and glide process and not exclusively by climb. Some of the glide could be produced by quenching strains. The quench-deformation experiment

(Fig. 2) may also be taken as evidence for the degeneration of helices into loops. Uniform growth of helices in thin foils (see Fig. 3b) is expected to occur by the same process that was discussed for loop growth.

#### Acknowledgements

We wish to acknowledge helpful discussions with Professor J. Washburn and Dr. G. Saada and thank the United States Atomic Energy Commission for financial support.

#### References

- 1 F. J. Bradshaw and S. Pearson: *Phil. Mag.* **2** (1957) 570.
- 2 M. J. Whelan: *Electron Microscopy and Strength of Crystals*, eds. G. Thomas and J. Washburn, Interscience, New York (1962) (in press).
- 3 G. Thomas: *Phil. Mag.* **4** (1959) 1213.
- 4 G. Thomas and M. J. Whelan: *Phil. Mag.* **4** (1959) 511.
- 5 C. Panseri and T. Federighi: *Acta Met.* **8** (1960) 217.
- 6 H. Kimura, A. Kimura and R. R. Hasiguti: *Acta Met.* **10** (1962) 607.
- 7 R. Bauer and V. Gerold: *Z. Metallk.* **52** (1961) 671.
- 8 P. B. Hirsch, J. Silcox, R. E. Smallman and K. H. Westmacott: *Phil. Mag.* **3** (1958) 897.
- 9 G. Thomas and M. J. Whelan: *Phil. Mag.* **6** (1961) 1103.
- 10 J. Silcox and M. J. Whelan: *Phil. Mag.* **5** (1960) 1.
- 11 W. M. Lomer: *Vacancies and Other Point Defects in Metals and Alloys*, Inst. of Metals Monograph and Report Series, London, **23** (1958).
- 12 R. Vandervoort and J. Washburn: *Phil. Mag.* **5** (1960) 24.
- 13 W. De Sorbo and D. Turnbull: *Acta Met.* **7** (1959) 83.
- 14 S. Amelinckx, W. Bontinck, W. Dekeyser and F. Seitz: *Phil. Mag.* **2** (1957) 355.
- 15 G. Saada and J. Washburn: *Proc. Int. Conf. Cryst. Latt. Def. (1962)*: *J. Phys. Soc. Japan* **18** Suppl. I (1963) 43.
- 16 W. Bontinck: *Phil. Mag.* **2** (1957) 561.
- 17 R. M. Emrick: *Phys. Rev.* **122** (1961) 1720.

#### DISCUSSION

**Lazarus, D.:** What justification do you have for writing  $E'_G = E_f + E_m - 2E_B$ ?

**Thomas, G.:** I have simply assumed that  $E_B$  appears equally with  $E_f$  and  $E_m$  which is not unreasonable in this case. The resultant value of  $E_B$  agrees well with our value obtained by comparing vacancy concentration ratios of Al-5% Mg and pure Al. The point is discussed in the paper.